Research in Astron. Astrophys. **2012** Vol. **12** No. **7**, 857–864
http://www.raa-journal.org *http://www.iop.org/journals/raa*

Research in Astronomy and Astrophysics

IPS observation system for the Miyun 50 m radio telescope and its commissioning observation

Xin-Ying Zhu[1], Xi-Zhen Zhang[1], Hong-Bo Zhang[1], De-Qing Kong[1] and Hui-Peng Qu[2]

[1] National Astronomical Observatories, Chinese Academy of Sciences, Beijing 100012, China; *zhuxy@bao.ac.cn*
[2] Beijing Institute of Tracking and Telecommunications Technology, Beijing 100094, China

Received 2011 December 20; accepted 2012 March 15

Abstract Ground-based observation of Interplanetary Scintillation (IPS) is an important approach for monitoring solar wind. A ground-based IPS observation system has been newly implemented on a 50 m radio telescope at Miyun station, managed by the National Astronomical Observatories, Chinese Academy of Sciences. This observation system has been constructed for the purpose of observing solar wind speed and the associated scintillation index by using the normalized cross-spectrum of a simultaneous dual-frequency IPS measurement. The system consists of a universal dual-frequency front-end and a dual-channel multi-function back-end specially designed for IPS. After careful calibration and testing, IPS observations on source 3C 273B and 3C 279 have been successfully carried out. The preliminary observation results show that this newly-developed observation system is capable of performing IPS observation. The system's sensitivity for IPS observation can reach over 0.3 Jy in terms of an IPS polarization correlator with 4 MHz bandwidth and 2 s integration time.

Key words: instrument — interplanetary scintillation — telescope — radio astronomy

1 INTRODUCTION

Interplanetary scintillation (IPS) is the random fluctuation in the intensity and phase of electromagnetic waves passing through interplanetary space. The fluctuation is caused by refraction and deflection from the inhomogeneous plasma (solar wind) in interplanetary space (Zhang 2007). Studying the solar wind impacts not only solar physics, space physics and geophysics, but also related fields, such as aerospace activities, space communications, the safety of humanity, and so on.

IPS observations with ground-based antennas have led to velocity estimates of the solar wind and structure estimates of distant compact radio sources (Hewish & Symonds 1969; Armstrong & Coles 1972). Such measurements, though indirect, reveal information from the ecliptic plane and close to the Sun, where direct spacecraft have not yet reached (Scott et al. 1983). Several important IPS stations are using ground-based telescopes for IPS observation, such as Cambridge (UK) (Hewish et al. 1964; Purvis et al. 1987), Ooty (India) (Swarup et al. 1971; Manoharan & Ananthakrishnan 1990), Puschino (Russia) (Vitkevich et al. 1976), STEL (Japan) (Asai et al. 1995) and MSRT (China) (Zhang et al. 2001; Wu et al. 2001). Many useful results have been produced by such observations.

In 2005, a megaproject of scientific research on space weather monitoring, namely the Meridian Space Weather Monitoring Project (Meridian Project for short), was approved by the Chinese government (Wang et al. 2009). As a group member of the Meridian Project, a ground-based IPS observation facility was sponsored and constructed with the objectives of observing solar wind speed and the associated scintillation index.

Two methods could be adopted to observe IPS using a single telescope. The first method is single-station, single-frequency (SSSF) observations (Hewish et al. 1964; Manoharan & Ananthakrishnan 1990; Liu et al. 2010). The second method is the single-station, dual-frequency (SSDF) method (Scott et al. 1983). According to preliminary studies (Zhang 2007), the SSDF technique has the following advantages over the SSSF method: (1) Higher accuracy in the calculation of the characteristic frequency; (2) Small effects from the variation of the solar wind parameters; (3) Higher sensitivity. The only additional cost for implementing the SSDF technique onto a 50 m radio telescope is development of the receiver. Efforts were thus made to build an IPS observation system with a dual-frequency front-end and dual-channel multi-function back-end to implement SSDF technology.

In this paper, we outline the IPS observation system in Section 2. IPS observations and results are given in Section 3. Finally, a preliminary conclusion on the IPS observation system is presented in Section 4.

2 OBSERVATION SYSTEM

Figure 1 illustrates the general layout of the IPS observation system as it relates to signal flow. The IPS observation system consists of a telescope system, front-end and back-end. When performing IPS observations, the telescope is aimed at the target radio source. The radio wave emitted by the radio source is collected and focused by the telescope and is then filtered by the selected working feed. The bandwidth-limited radio frequency (RF) signal is then amplified and down-converted to an intermediate frequency (IF) signal by the front-end. The IF signal effectively lowers the transmission

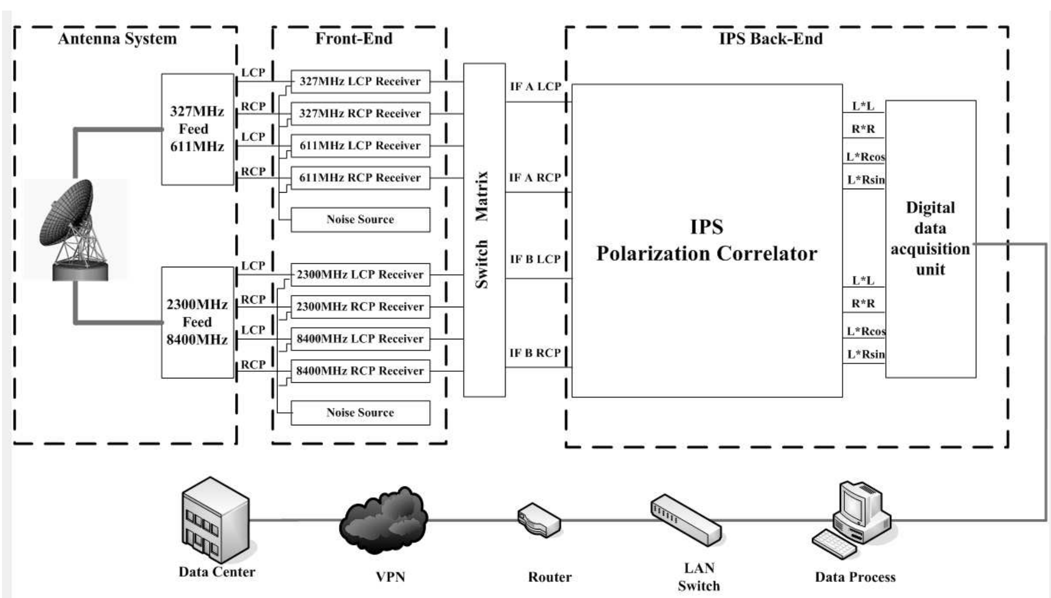

Fig. 1 Block diagram of the IPS observation system.

Table 1 Technical Data Describing the Telescope

Reflector Diameter	50 m
Aperture	1099 $m^2(S)$, 852 $m^2(X)$, 1119 m^2(327 MHz), 1119 m^2(611 MHz)
Pointing Accuracy	$19''$
Azimuth Range	$-270° \sim +270°$
Maximum Rotation Speed	$60°\ min^{-1}$
Elevation Range	from 7° to 88°
Maximum Tilt Speed	$30°\ min^{-1}$
Total Weight	640 t
Optics Prime focus	$F/D = 0.35$

losses as the signal passes through coaxial cables. The switch matrix is used to adjust the input and output at one's discretion. Each of two IF signals representing two polarizations of one working frequency are connected to one IPS polarization correlator. After power detection and correlation, four components of input IF signals (L*L, R*R, L*Rcos, L*Rsin) are produced. Output components of the IPS polarization correlator are then converted from an analog signal to a digital signal and recorded by a digital data-acquisition unit as original observation data. After being processed by a computer, both original observation data and preliminary scientific parameters such as solar wind speed and the scintillation index are transferred to the data center through a network. The system's sensitivity for IPS observation can reach over 0.3 Jy in terms of the IPS polarization correlator with a 4 MHz bandwidth and 2 s integration time.

2.1 TELESCOPE SYSTEM

The 50 m Radio Telescope, which is now the biggest radio telescope in China, was built in 2006 for the Chinese Lunar Exploration project. The telescope is located about 1.5 km south of the village of Bulaotun, in the north part of Miyun county. In the vicinity of the telescope is the Miyun reservoir, which is the most important water source for the capital, with a designed water-storage capacity of 4.3 billion cubic meters. The telescope and the reservoir are surrounded by mountains, which provide a good electromagnetic environment for the telescope by preventing radio frequency interference (RFI) from surrounding sources.

The 50 m radio telescope is operated by the National Astronomical Observatories, Chinese Academy of Sciences (NAOC). Like most of the other large radio telescopes around the world, it has an altitude-azimuth mounting. The whole telescope is mounted on wheels on a circular track, and the dish moves about a horizontal axis between the two A-shaped beams. The parabolic reflector is made from a solid filled panel in the inner 30 m region and wire mesh in the outer part. All receivers and feeds are located at the prime focus. The 50 m radio telescope is shown in Figure 2 and the technical data describing the telescope are listed in Table 1 (Zhang et al. 2009).

2.2 Front-end

According to the design of the IPS observing system, the IPS front-end requires a total of eight sets of receivers, four sets for the S/X dual-band feed and another four sets for the UHF dual-band feed. Up to four of the eight sets of receivers could be simultaneously used in observations to meet different scientific needs. Due to financial constraints, three existing receivers are used for the S/X band, two room temperature receivers are for the S band and one cryogenic receiver is for the X band. Four new UHF receivers have already been developed, and will be installed on the telescope after the Chang-E II mission next year. All available receivers for the IPS front-end are shown in Figure 3 and the specifications for each receiver are listed in Table 2.

Table 2 Main Specifications of the Front-End

No.	Item	S band	X band	UHF (327 MHz)	UHF (611 MHz)
1	Frequency Range	2150–2450 MHz	8200–9000 MHz	307–347 MHz	591–631 MHz
2	Gain	$\geq$ 65 dB	$\geq$ 65 dB	$\geq$ 65 dB	$\geq$ 65 dB
3	Receiver Noise Temperature	$\leq$ 50 K	$\leq$ 20 K	$\leq$ 55 K	$\leq$ 55 K
4	IF	550–850 MHz	100–900 MHz	307–347 MHz	591–631 MHz
5	Polarization	LCP&RCP	RCP	X&Y	X&Y

Fig. 2 50 m telescope at Miyun station.

Fig. 3 Front-end of the IPS observation system.

2.3 Back-end

A dual-channel multi-function back-end is designed exclusively for IPS observation. The back-end consists of a polarization correlator and a digital data acquisition unit; the block diagram of the back-end is shown in Figure 4. The input signal to the polarization correlator is down-converted and

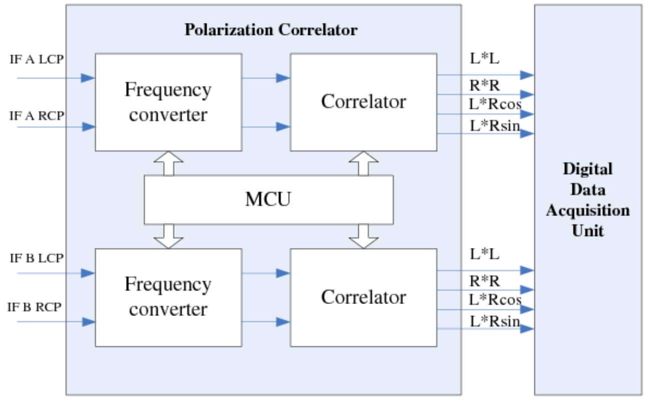

Fig. 4 Block diagram showing the components of the IPS back-end unit.

amplified to make sure that the mixer works at its optimal performance. In order to prevent RFI, the local oscillator frequency of the mixer and signal bandwidth can be chosen according to the specific need of the observation. In addition, the integration time can also be adjusted between 10 ms to 2 s with a step size of 10 ms. Four output components (L*L, R*R, L*Rcos, L*Rsin) are produced after the correlation of every two input signals (L, R). Virtual instrument technology which consists of a workstation equipped with powerful application software and a plug-in sample board is used to perform the functions of a digital data acquisition unit. The analog signal output by the polarization correlation is captured by the plug-in sample board through its I/O port, then the captured signal is converted from an analog signal to a digital signal by an A/D converter. After the A/D conversion, the signal is stored in a FIFO buffer to form a data block. The workstation equipped with this plug-in sample board reads the data blocks via the USB bus at regular intervals, then makes the necessary calculations and saves the data according to the user-defined format.

3 OBSERVATIONS AND RESULTS

In 2011 September, commissioning observations of the new IPS observation system were conducted at Miyun station after a period of system testing, debugging and optimization. The IPS observation system intended to monitor solar wind speed and the scintillation index is capable of working in SSSF mode and SSDF mode. During SSSF mode, either 327 MHz, 611 MHz, 2300 MHz or 8400 MHz could be selected as the working frequency. During SSDF mode, both the 327 MHz/611 MHz frequency group and the 2300 MHz/8400 MHz frequency group could be selected to conduct the observations in turn. Since the scintillation decreases sharply at high frequency, strong sources such as 3C 273B and 3C 279 are chosen for the commissioning observations. The radiation spectrum of 3C 273B and 3C 279 is flat, which means that the source's flux density for 2300 MHz is almost the same value as for 8400 MHz. The key parameters of the commissioning observation with the new IPS observation system are listed in Table 3.

When radio waves emitted from distant sources pass through interplanetary space, the intensity and phase of the radio wave will scintillate because of interactions with the solar wind. The scintillation, which carries a variety of physical information on the spatial distribution of space plasma, is proportional to the negative fourth power of the heliocentric distance. The distance at which the weak scintillation regime sets in is a function of frequency (see Table 4). From Table 4, short wavelengths are necessary for observations closer to the Sun and are much more difficult to observe compared to long wavelengths. For this reason, the ability to detect the changes of received radio signals with

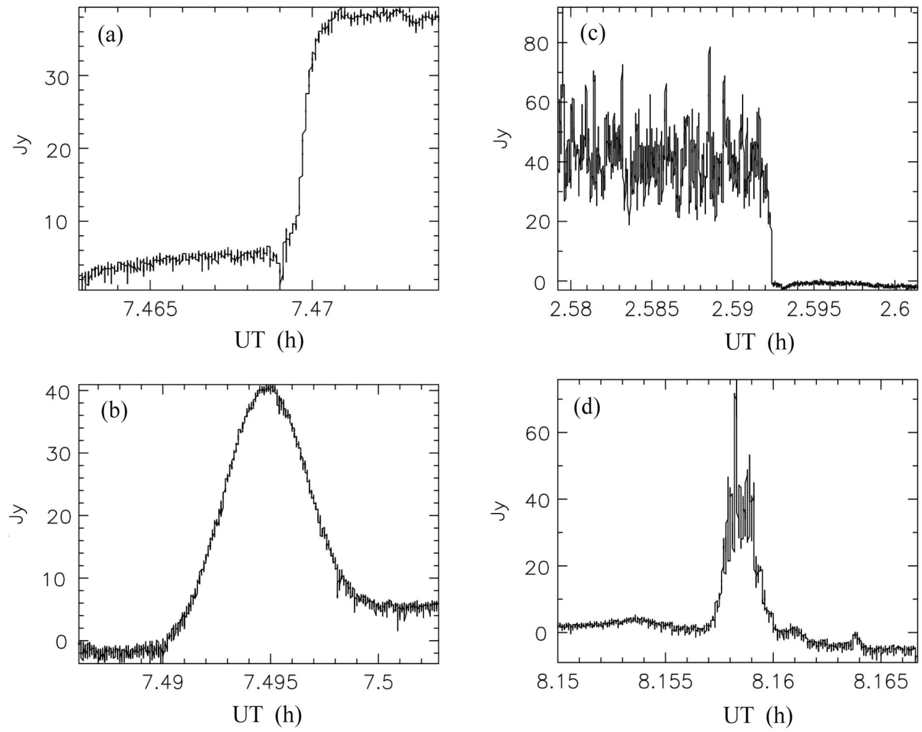

Fig. 5 (a) and (b): Raw observation data from 3C 273B on 2011 October 27, and (c) and (d): Raw observation data from 3C 273B on 2011 September 27. The ordinate displays the power and the abscissa displays the UTC, which are scaled linearly as 2 Jy per division and 0.001 hour per division, respectively).

Table 3 Key Parameters of Commissioning Observations with the New IPS Observing System (Telescope: Miyun 50 m Radio Telescope)

Observation Date	2011–09–20∼2011–09–29	2011–10–12∼2011–10–20
Source/Flux	3C 273B/41 (Jy)	3C 279/12 (Jy)
Frequency/Bandwidth	2300 MHz/80 MHz	8400 MHz/80 MHz
Minimum Distance from Sun	3C 273B/18 $R_\odot$	3C 279/15 $R_\odot$
Sample Time	Hardware 1 ms	Software 10 ms
Shortest Integrated Time	240 s	

Table 4 Minimum Distance the Weak Scintillation Condition Begins to Hold as a Function of Frequency

Frequency (MHz)	150	327	900	2000	5000	7500	20000
Heliocentric distance ($R_\odot$)	60	35	18	10	5	4	2

short wavelengths is an important criterion to verify the integrity of the whole IPS observation system. The raw S-band data from the IPS observation system are shown in Figure 5.

In Figure 5(a), we show the raw OFF-ON data from 3C 273B acquired on 2011 October 27 (OFF: The telescope keeps track of the target with a constant deviation in the targeting position from it; ON: The telescope keeps track of the target by staying pointed at it). At this time, the

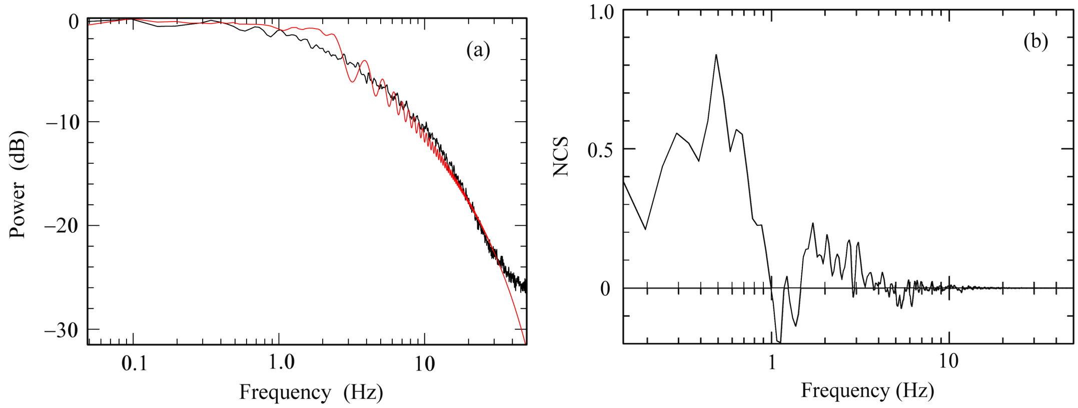

Fig. 6 (a) IPS spectrum of observation data from 3C 273B on 2011 September 27 (The red line is the theoretically fitted curve, *color online*). (b) Normalized co-spectrum (NCS) between the pairs of radio frequencies 2300/8400 in MHz. Scales are logarithmic for frequency and power density (2 dB per division) and linear for NCS.

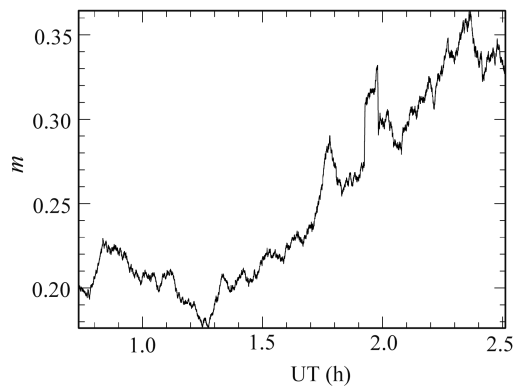

Fig. 7 Scintillation index of observation data from 3C 273B on 2011 September 27.

angular distance between 3C 273B and the Sun is large and the observation data show that the noise fluctuations of the received signal are almost the same when different modes of OFF or ON are applied, and the signal received by the observation system is stable without RFI.

In Figure 5(c), the raw OFF-ON data from 3C 273B on September 27 are presented. Because 3C 273B is close to the Sun at this time, great differences between the OFF-ON noise fluctuations of the received signal are observed. When the telescope targets 3C 273B in OFF mode, the noise fluctuation of the received signal is small, only reflecting the system's own noise fluctuation. When the telescope targets 3C 273B in ON mode, the severe fluctuation of the received signal strength shows that the radio signal emitted by 3C 273B has been scintillated by solar wind. Comparison of Figure 5(a) and (c) proves that the newly developed IPS observation system has the ability to observe interplanetary scintillation. Figure 5(b) and (d) shows raw data when the telescope scanned 3C 273B on October 27 and September 27 respectively. The noise fluctuation of the whole telescope beam is almost the same as in Figure 5(b) but the main lobe fluctuates severely in Figure 5(d) because of the scintillation caused by solar wind. The observation data of 3C 273B on 2011 September 27 are used to perform data analysis. After preliminary data processing, an IPS spectrum and a normalized cross-spectrum (NCS) of pairs of radio frequencies 2300 MHz/8400 MHz are obtained. The IPS power spectrum of 2300 MHz is shown in Figure 6(a), in which the red line represents the theoretically fitted curve.

Figure 6(b) shows the NCS of the pairs of radio frequencies 2300 MHz/8400 MHz. According to the theoretically fitted curve, the solar wind speed is about 630 km s^{-1} in the direction perpendicular to the line of sight. The scintillation index of this observation is shown in Figure 7.

4 CONCLUSIONS

According to preliminary results, the newly developed IPS observation system is now capable of performing interplanetary scintillation observations.

Acknowledgements This work was funded by the Meridian Space Weather Monitoring Project.

References

Armstrong, J. W., & Coles, W. A. 1972, J. Geophys. Res., 77, 4602
Asai, K., Ishida, Y., Kojima, M. et al. 1995, J. Geomag. Geoelectr., 47, 1107
Hewish, A., Scott, P. F., & Wills, D. 1964, Nature, 203, 1214
Hewish, A., & Symonds, M. D. 1969, Planet. Space Sci., 17, 313
Liu, L.-J., Zhang, X.-Z., Li, J.-B., et al. 2010, RAA (Research in Astronomy and Astrophysics), 10, 577
Manoharan, P. K., & Ananthakrishnan, S. 1990, MNRAS, 244, 691
Purvis, A., Tappin, S. J., Rees, W. G., Hewish, A., & Duffett-Smith, P. J. 1987, MNRAS, 229, 589
Scott, S. L., Rickett, B. J., & Armstrong, J. W. 1983, A&A, 123, 191
Swarup, G., Sarma, N. V. G., Josshi, M. N., et al. 1971, Nature Physical Science, 230, 185
Vitkevich, V. V., Glushaev, A. A., Iliasov, I. P., et al. 1976, Radiofizika, 19, 1594
Wang, C., Feng, X., Wan, W. X., et al. 2009, Recent Developments in World Seismology (in Chinese), 6, 32
Wu, J., Zhang, X., & Zheng, Y. 2001, Ap&SS, 278, 189
Zhang, X.-Z. 2007, ChJAA (Chin. J. Astron. Astrophys.), 7, 712
Zhang, X. Z., Wu, J. H., Chen, H. S., et al. 2001, Kexue Tongbao (in Chinese), 46, 1081
Zhang, X.-Z., Zhu, X.-Y., Kong, D.-Q., et al. 2009, RAA (Research in Astronomy and Astrophysics), 9, 367